

# Stimulated emission in ridge quantum wire laser structures measured with optical pumping and microscopic imaging methods

Shinichi Watanabe,<sup>a)</sup> Shyun Koshiba,<sup>b)</sup> Masahiro Yoshita, Hiroyuki Sakaki,<sup>b)</sup> Motoyoshi Baba, and Hidefumi Akiyama

*Institute for Solid State Physics, University of Tokyo, 7-22-1 Roppongi, Minato-ku, Tokyo 106-8666, Japan*

(Received 24 March 1998; accepted for publication 26 May 1998)

We report the observation of stimulated emission in ridge quantum wire (QWR) structures at temperatures from 4.7 to 290 K. To examine the origin of the stimulated emission, the spatially and spectrally resolved microscopic images of the emission were measured. It was most likely attributed to the optical transition between the excited states in QWRs. © 1998 American Institute of Physics. [S0003-6951(98)04230-2]

Quantum wire (QWR) semiconductor lasers with novel one-dimensional (1D) properties have attracted great attention. Due to the peaked structure of the 1D density of states (DOS), reduced temperature dependence<sup>1,2</sup> and low threshold current density<sup>2,3</sup> have been predicted.

Kapon *et al.*<sup>4</sup> reported the first observation of stimulated emission in QWRs using V-groove structures. Their emission was due to the transition between QWR higher subbands, or the excited states of QWRs. Wegscheider *et al.*<sup>5</sup> reported stimulated emission from the ground state exciton in T-shaped QWRs.

In this letter, we report the investigation of stimulated emission in ridge QWR structures by optical pumping. Since the ridge QWR structures have some advantages in making large lateral confinement energy and high crystal quality,<sup>6,7</sup> they are promising to realize room-temperature QWR lasers with novel properties inherent in the 1D system. We investigate the positions and patterns of the stimulated emission, using a microscopic imaging technique.<sup>8</sup>

A cross-sectional scanning-electron-microscope (SEM) image of a ridge QWR structure (sample A) is shown in Fig. 1. The sharp ridge structure was formed via the facet growth of GaAs by molecular beam epitaxy (MBE) on a patterned GaAs (001) substrate with lines and spaces of 2.0  $\mu\text{m}$  width.<sup>6,7</sup> The curvature of the ridge top was controlled by the growth condition to have a lateral width of 10–20 nm.<sup>9</sup>

On top of the ridge structures, separately confined-heterostructure (SCH) layers were formed. The core layer of the SCH was composed of a GaAs active layer with a nominal vertical thickness of 5 nm sandwiched by 90 nm thick barrier layers of a  $\text{Al}_{0.2}\text{Ga}_{0.8}\text{As}$  digital alloy. As a result, GaAs quantum wells (QWs) denoted as side-QWs in Fig. 1 were formed on (111)B facets and had  $5/\sqrt{3}$  nm thickness. On the other hand, the curved 10–20 nm wide region on the ridge top had 5 nm thickness, which realized 1D electronic states called ridge QWRs.

The core layer was sandwiched by the cladding layers of the  $\text{Al}_{0.4}\text{Ga}_{0.6}\text{As}$  digital alloy to construct SCH optical

waveguides. After the MBE growth, the sample was cleaved into  $L=300 \mu\text{m}$  in length perpendicularly to the ridge QWRs to form an optical cavity. In a similar way, two samples B and C were also prepared, which will be described later.

Sample A was then characterized by photoluminescence (PL) spectroscopy and imaging measurements. Optical excitation was performed by the second harmonics of continuous-wave mode-locked yttrium-lithium fluoride (YLF) laser pulses with a wavelength of 526 nm, repetition rate of 75.4 MHz, and pulse duration of 50 ps. The pump laser light was incident on the top of the ridge structures as shown in Fig. 1. It was focused via two cylindrical lenses into a stripe region which covered several wire structures uniformly. The PL was collected from one of the cleaved edges by a lens, and led to the detection system for spectroscopy and imaging described in a separate article.<sup>8</sup>

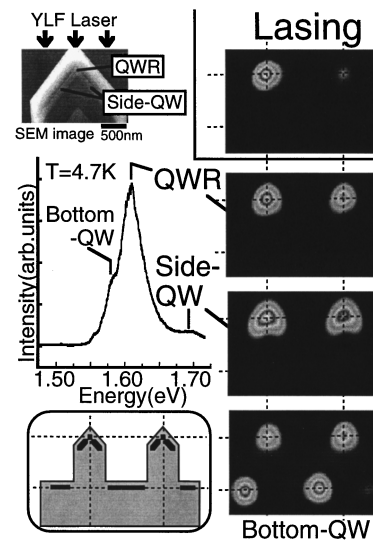


FIG. 1. SEM cross-sectional image of sample A, and its spectrally and spatially resolved cross-sectional PL contour-plot images (4.7 K), corresponding to the three spectral peaks in the PL spectrum for the pump power of 2  $\text{W}/\text{cm}^2$ . Each spectral peak is assigned as QWRs (1.610 eV), side-QWs (1.699 eV) and bottom-QWs (1.584 eV) by its emission pattern. Image of stimulated emission at 1.687 eV is also shown (indicating as "Lasing") for the pump power of 0.7  $\text{kW}/\text{cm}^2$ . Note that the lasing image is centered at the top of the ridge structure, similarly to the PL image of the QWRs.

<sup>a)</sup>Electronic mail: watanabe@wagner.issp.u-tokyo.ac.jp

<sup>b)</sup>Quantum Transition Project, Japan Science and Technology Corporation and Research Center for Advanced Science and Technology, University of Tokyo, 4-6-1 Komaba, Meguro-ku, Tokyo 153-8904, Japan.

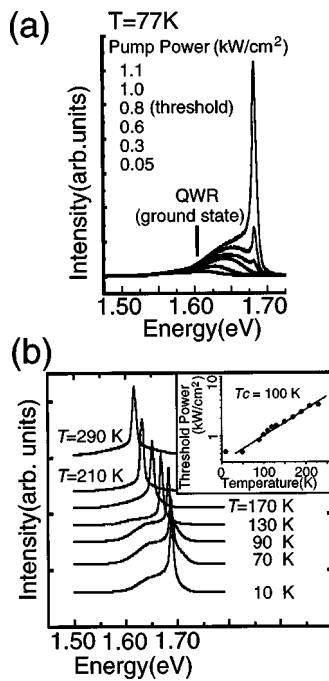


FIG. 2. (a) PL spectra at 77 K for the various excitation powers of 0.05, 0.3, 0.6, 0.8, 1.0 and 1.1  $\text{kW/cm}^2$ . The sharp lines due to stimulated emission are observed at 1.682 eV above the threshold power of 0.8  $\text{kW/cm}^2$ . (b) Temperature dependence of stimulated emission spectrum from 10 to 290 K. The spectral peak shift of lasing energy is mainly caused by that of the band-gap energy with temperature. The inset shows the temperature dependence of the threshold pump power for stimulated emission, from which the characteristic temperature is estimated to be 100 K as the slope of the semilog plot.

The PL spectrum of sample A at 4.7 K for a weak pump power of  $2 \text{ W/cm}^2$  (average power) is shown in Fig. 1. Three spectral peaks were observed at 1.699, 1.610, and 1.584 eV. The PL image at each PL peak energy with a band width of 2 nm was then measured with an interference filter, and is shown as a contour-plot image in Fig. 1. The spatial resolution of the measurement was about  $1 \mu\text{m}$ .<sup>8</sup>

The image of the PL at 1.610 eV showed that the PL originated from the top of ridge structures, and hence from the QWRs. The image of the PL at 1.699 eV followed the geometry of side-QWs, so that the PL peak was attributed to the side-QWs. Note here that the energy level of the QWRs was lower than the side-QWs by 90 meV, showing that the well stabilized 1D ground state was realized, as was confirmed in our previous studies.<sup>6,7</sup> Between the two levels, we expected several higher subbands in QWRs. However, their theoretical estimation requires more precise structural characterization of the ridge shape,<sup>10</sup> which is the subject of future study.

It also turned out that the image at the PL energy of 1.584 eV was composed of PL from bottom-QWs, or QWs formed at valleys between the ridge structures, and PL from QWRs. Though this energy was lower than the energy levels of QWRs and side-QWs, the bottom-QWs were isolated from them, and hence, independent of the emission processes in QWRs.

The excitation intensity dependence of PL spectra of sample A immersed in liquid nitrogen at 77 K is shown by the six curves in Fig. 2(a). When the pump power was relatively weak ( $< 0.05 \text{ kW/cm}^2$ ), the PL peak of QWRs was

observed at 1.606 eV, while the PL of the side-QWs was very weak at this temperature.

As the pump power was increased, the low-energy side of the QWR PL peak became saturated, and the higher-energy region increased to make the spectral peak blue-shifted. This spectral shift indicated the saturation of electrons and holes in the ground states in QWRs and the increased occupation of excited states in QWRs. Note that a higher PL intensity was observed in the excited states in QWRs than that of the ground states, which indicated that the DOS became higher at higher energy in QWRs. Considering the saw-tooth-like 1D DOS, this was most likely attributed to the higher subbands in QWRs.

Finally, at a pump power of  $0.8 \text{ kW/cm}^2$ , stimulated emission was observed at 1.682 eV. The lasing energy was higher by 76 meV than the ground-state PL energy of QWRs. Note, however, that it was still below the energy level of the side-QWs, which was 90 meV above the ground state of the QWRs. Therefore, the stimulated emission was not to be attributed to optical transition in the side-QWs, but to the transition between the excited states in the QWR higher subbands.

This fact was further confirmed by the imaging measurement of stimulated emission. Indicated as "Lasing" in Fig. 1 is the image of stimulated emission observed at 1.687 eV for the above-threshold pump power of  $0.7 \text{ kW/cm}^2$  at 4.7 K. Note that the image of the stimulated emission was centered at the top of the ridge structure, similarly to the PL pattern from the QWRs. Although the emission pattern should be partly affected by a waveguide structure, this observation supports our assignment that the origin of the stimulated emission was the optical transition between the high-energy excited states in the QWRs.

Temperature-dependent PL and stimulated-emission measurements were also performed. Figure 2(b) shows the spectrum of stimulated emission at each temperature. Lasing was observed at all the temperatures between 4.7 and 290 K. The lasing energy became gradually lower for higher temperatures. The change in the lasing energy was mainly caused by that of the band-gap energy with temperature, so that the origin of the lasing was considered unchanged. The temperature dependence of the threshold pump power for stimulated emission is also shown in the inset of Fig. 2(b), from which the characteristic temperature was estimated to be 100 K as the slope of the semilog plot.

The values of the threshold excitation power were rather large especially at high temperatures. One of the reasons is the substantial amount of loss occurring in the initial carrier capture process. A large portion of initially generated carriers in barrier layers undergo surface recombination or other decay processes before they are captured in QWRs.

Another reason is the broadened DOS at the band edge due to the structural inhomogeneity of the QWRs. In the regime where electrons and holes are saturated in their states, gain is limited by the DOS. Improvement of this factor is important not only to reduce the laser threshold, but also to achieve ground subband lasing in QWRs.

In fact, when the optical cavity length of the sample was increased to  $L = 1 \text{ mm}$ , the lasing occurred at the slightly lower energy, 1.663 eV, at 77 K. This shows that the re-

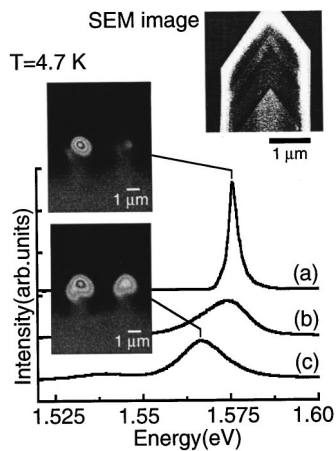


FIG. 3. PL spectra and corresponding PL contour-plot images of sample B at 4.7 K for the pump powers of (a) 1.6 kW/cm<sup>2</sup>, (b) 240 W/cm<sup>2</sup>, and (c) 5 W/cm<sup>2</sup>. The images are measured at (a) 1.576 eV (lasing) and (c) 1.566 eV (side-QW). The images are presented on the weak background reflection images of sample B with tungsten-lamp illumination. The lasing image shows that the right part of the side-QW is the origin of the stimulated emission. The SEM cross-sectional image is also shown.

quired gain for lasing was achieved at relatively lower excited states with a slightly lower DOS because of the increased length of the active region.

It is interesting to compare these observations on sample A with that of the two other ridge-structure samples B and C. The nominal vertical thicknesses of GaAs active layers were 9 nm (sample B) and 11 nm (sample C) instead of 5 nm (sample A). The cavity lengths of samples B and C were 300 μm and 1 mm, respectively. Though the other parameters were set identical, the SEM images presented in Figs. 3 and 4 have shown that the ridge structures of sample B were asymmetric, and the ridge top of sample C was flat with 100 nm width to have QWs (top-QWs), instead of QWRs, with 11 nm thickness.

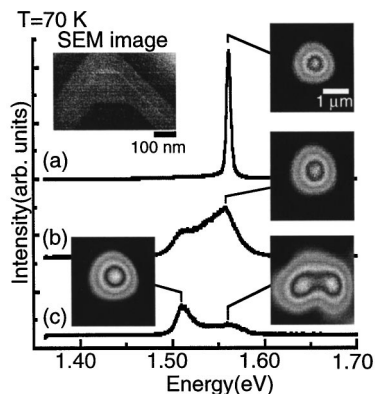


FIG. 4. PL spectra and corresponding PL contour-plot images of sample C at 70 K, for the pump powers of (a) 1.9 kW/cm<sup>2</sup>, (b) 1.3 kW/cm<sup>2</sup>, and (c) 150 W/cm<sup>2</sup>. The images are measured at (a) 1.561 eV (lasing), (b) 1.558 eV (the excited state of the top-QW), (c) 1.509 eV (top-QW) and 1.560 eV (side-QW). The lasing image shows that the excited state of the top-QW is the origin of the stimulated emission. The SEM cross-sectional image is also shown.

Figure 3 shows PL spectra and corresponding PL contour-plot images of sample B at 4.7 K, with its cross-sectional SEM image. Under a weak pump power [(c) 5 W/cm<sup>2</sup>], two PL peaks were observed from side-QWs (1.566 eV) and QWRs (1.539 eV). As the pump power was increased [(b) 240 W/cm<sup>2</sup>], the PL of the side-QWs grew in intensity and blueshifted, and then lasing occurred at 1.575 eV [(a) 1.6 kW/cm<sup>2</sup>]. The image of the stimulated emission shows that it comes from the region of the right part of the side-QW. This is the case that the side-QW is the origin of the stimulated emission.

Figure 4 shows PL spectra and corresponding PL contour-plot images of sample C at 70 K, with its cross-sectional SEM image. Under weak pump power [(c) 150 W/cm<sup>2</sup>], the PL peak energy of the side-QWs was 1.560 eV, at which the images of the left and right side-QWs were separately observed. The PL peak of the top-QW was observed at 1.509 eV. At high pump power [(a) 1.9 kW/cm<sup>2</sup>], the stimulated emission occurred at 1.561 eV. Note in the PL image that PL at 1.561 eV was dominated by PL from the top-QW at high pump power [(b) 1.3 kW/cm<sup>2</sup>], and that the stimulated emission came from the top-QW region. Thus, the origin of the stimulated emission should be attributed to the transitions between the excited states of the top-QWs, even if the energy of the stimulated emission was at the same energy as the PL of the side-QWs at the weak pump power.

These two examples further support the assignment of the origin of the stimulated emission on the basis of its emission image.

In summary, stimulated emission was observed in ridge QWR laser structures from 4.7 to 290 K. The origin of the stimulated emission was most likely the transitions between excited states in the higher subbands of the QWRs. The emission image centered at the position of the QWRs assisted such a conclusion.

This work is partly supported by a Grant-in-Aid from the Ministry of Education, Science, Sports, and Culture, Japan, and the Ogasawara Foundation for the Promotion of Science and Engineering.

<sup>1</sup> Y. Arakawa and H. Sakaki, *Appl. Phys. Lett.* **40**, 939 (1982).

<sup>2</sup> Y. Arakawa and A. Yariv, *IEEE J. Quantum Electron.* **22**, 1887 (1986).

<sup>3</sup> M. Asada, Y. Miyamoto, and Y. Suematsu, *Jpn. J. Appl. Phys., Part 2* **24**, L95 (1985).

<sup>4</sup> E. Kapon, D. M. Hwang, and R. Bhat, *Phys. Rev. Lett.* **63**, 430 (1989).

<sup>5</sup> W. Wegscheider, L. N. Pfeiffer, M. M. Dignam, A. Pinczuk, K. W. West, S. L. McCall, and R. Hull, *Phys. Rev. Lett.* **71**, 4071 (1993).

<sup>6</sup> S. Koshiba, H. Noge, H. Akiyama, T. Inoshita, Y. Nakamura, A. Shimizu, Y. Nagamune, M. Tsuchiya, H. Kano, and H. Sakaki, *Appl. Phys. Lett.* **64**, 363 (1994).

<sup>7</sup> H. Akiyama, S. Koshiba, T. Someya, K. Wada, H. Noge, Y. Nakamura, T. Inoshita, A. Shimizu, and H. Sakaki, *Phys. Rev. Lett.* **72**, 924 (1994); **72**, 2123 (1994).

<sup>8</sup> M. Yoshita, H. Akiyama, T. Someya, and H. Sakaki, *J. Appl. Phys.* **83**, 3777 (1998).

<sup>9</sup> S. Koshiba, I. Tanaka, Y. Nakamura, I. Kamiya, T. Someya, T. Ngo, and H. Sakaki, *J. Cryst. Growth* **175-176**, 804 (1997).

<sup>10</sup> T. Inoshita and H. Sakaki *J. Appl. Phys.* **79**, 269 (1996).